

LUMINESCENCE STUDIES ON PZT:Eu³⁺ SOL-GEL THIN FILMS.

Jorge Garcia-Macedo^{1}, Jesús A. Martínez Zuñiga¹, Federico Gonzalez-Garcia², Guadalupe Valverde-Aguilar¹*

1. Instituto de Física, UNAM. P.O. Box 20-364, 01000 México D.F. Phone: + (55) 56 22 51 03; fax: + (55) 56 22 50 11. E-mail: gamaj@fisica.unam.mx
2. Instituto de Investigaciones en Materiales, Circuito Investigación Científica S/N, Ciudad Universitaria, México D.F.

ABSTRACT

PZT: Eu³⁺ sol-gel thin films and bulk samples were synthesized by sol-gel method. The crystalline structure (perovskite) was obtained in these materials by heat treatment at different temperatures. The temperature for the films was lower than that used in the bulk samples to obtain the perovskite-type phase. X-ray diffraction shows the presence of the perovskite phase in both kinds of materials. Emission and excitation studies of the impurity Eu³⁺ were made to determine its luminescence response. For PZT: Eu³⁺ thin films, the excitation spectra shows a broad band from charge transfer and narrow peaks due to the ${}^7F_0 \rightarrow {}^5L_6$ and ${}^7F_1 \rightarrow {}^5D_3$ transitions with $\lambda_o=612$ nm; and due to ${}^7F_0 \rightarrow {}^5L_6$ and ${}^7F_0 \rightarrow {}^5D_2$ with $\lambda_o=650$ nm. The films exhibit a PZT pyrochlore phase. The decays show two general components: a fast one and a slow one. The bulk samples do not have the PZT pyrochlore phase, but a tetragonal phase was detected. They show hypersensitive transitions as ${}^7F_0 \rightarrow {}^5D_2$ (excitation) and ${}^5D_0 \rightarrow {}^7F_2$ (emission). These transitions reveal the presence of Eu³⁺ in sites of low symmetry.

In the bulk sample the luminescence decrease at 300 °C, and disappear at higher temperature. It was recovered at 1000 °C. Instead, the thin film recovers its luminescence at 600 °C. This inhibition of the luminescence could be associated with the crystallite size formed in the samples.

The PZT: Eu³⁺ thin films show several advantages in comparison to the bulk samples, as a short time of preparation, and a better perovskite phase obtained at lower temperature.

Keywords: sol-gel, rare earth, luminescence, PZT.

1. INTRODUCTION.

The photoluminescence (PL) of rare-earth (RE, or lanthanide) ions in glassy matrices is of high technological importance, namely when it involves stimulated emission of radiation in laser and amplifier devices¹. The study of the luminescent properties of trivalent lanthanides incorporated into several crystalline matrices, is strongly motivated because of their technological applications in optoelectronics devices and flat panel displays. Then, it is important the systematic research of the RE hosted in different kind of matrices with good mechanical and thermal properties and chemical stability.

Although a number of important papers concerning the effect of trivalent rare earths on the electrical and structural properties of PZT have been published²⁻⁶, there are no studies reported on luminescence in these materials. This is probably due to the bulk PZT opacity. On the other hand, there are reports on the optical properties of the material and its potential applications, mainly in the form of thin films⁷⁻⁹, in which the doped rare earth ions open up new possibilities. An important advantage is that the fluorescence properties of the dopants enable us to study the microstructure.

The sol-gel method, based on wet chemistry processing, is quite cheap and simple for the fabrication of thin films and bulk samples, where significant RE ion concentrations, in particular Eu³⁺, can be achieved¹⁰.

In the present work, we synthesized two kinds of PZT samples by the sol-gel technique: thin films and bulk samples. Photoluminescence response of Eu³⁺ ions (at 1% molar weight) in Pb(Zr_xTi_{1-x})O₃ (PZT) polycrystalline is reported. The crystalline structure of the compound was obtained by X-Ray diffraction and corresponds to the space

group Pbcn. The time resolved luminescent spectra shown two aggregation types of Eu³⁺ into PZT samples, corresponding with two different exponential decays.

We discuss about the origin of the aggregation types of europium and the importance of symmetry on the Eu³⁺ transition lifetimes.

2. EXPERIMENTAL SECTION.

Materials Preparation

Acetate alkoxide gels with composition $\text{PbZr}_{0.47}\text{T}_{0.53}\text{O}_3$ were prepared from lead acetate trihydrate $\text{Pb}(\text{CH}_3\text{COO})_2 \cdot 3\text{H}_2\text{O}$ (99.9+%), europium(III) nitrate pentahydrate $\text{Eu}(\text{NO}_3)_3 \cdot 5\text{H}_2\text{O}$ (99.9%), zirconium propoxide $\text{Zr}(\text{C}_3\text{H}_7\text{O})_4$ (70% in 1-propanol) and titanium isopropoxide $\text{Ti}[(\text{CH}_3)_2\text{CHO}]_4$ (99.999%). Glacial acetic acid (99.8%) and tridistilled water were used as solvents, using the modified process from Yi *et al.*¹¹.

The bulk samples were obtained by using the experimental method reported by González *et al.*¹⁰ and co-workers. The previous solution was dried at room temperature for several weeks. The dried powdered gels were annealed at 200, 400, 500 and 700°C for 1 h. After these treatments, the powders were cold pressed to form pellets under a 3 ton load using an uniaxial hydraulic press. The pellets were then treated at 900 and 1000°C for 1 h.

Thin films were prepared by using the previous solution, too. Glass substrates were cleaned with deionized water (DI) under stirring twice times. After, the substrates were washed with soap and water to be deposited in a flask with acetone under stirring twice times again. Finally, the substrates were dried with compressed air and they were annealed at 300 °C. The dimensions of the glass substrates were 1 cm². Films were deposited on the glass substrates by spin-coating technique at rate of 3000 rpm for 20 seconds. A pyrolysis process at 300 °C for 10 minutes was done five times to deposit five coats on the substrates.

Characterization

The crystalline structure of the compound was obtained by x-ray diffraction with a Siemens D5000 powder diffractometer working at 30 kV–20 mA and equipped with a graphite monochromator previously attached to the secondary beam arm of the goniometer. A step-scanning mode with a step of 0.02° in the range from 5 to 70° in 2θ and an integration time of 2 s was used. We worked with the CuK radiation as the primary beam. Emission and excitation optical spectra were collected at room temperature with a SPEX FLUOROLOG FL111 spectrofluorimeter equipped with a 150W xenon lamp. Lifetimes were measured with this system but using a pulsed Xe lamp (40μs pulses) and its phosphorimeter. Excitation and emission wavelengths were selected by two monochromators (SPEX spectrometer 0.34m), and the detection was done with a HAMAMATSU R928 photomultiplier tube.

Transmission electron microscopy (TEM) analysis was performed on ground pieces obtained from the pellets, mounted on carbon-coated grids, in a JEOL 4000EX high resolution TEM (HRTEM) at 400 kV with 0.17 nm resolution.

3. RESULTS AND DISCUSSION.

X-ray diffraction. Figure 1 shows the XRD patterns for thin films doped Eu³⁺ ions annealed at a) 500° C, b) 550° C y c) 600° C. The evolution shows a maximum diffraction peak around 2θ = 30°, which corresponds to the pyrochlore phase. This phase is transitory during crystallization¹². This behaviour is reported in PZT thin films obtained by *sputtering* technique¹³. The peaks at 2θ = 22.2° and 2θ = 31.6° corresponding to the (100) and (110) peaks, respectively, denote the initial formation of the perovskite structure (Figure 1 (b)). The peaks at 2θ = 29.65° (222) and 34.6° (400) indicate the presence of pyrochlore phase. The tetragonal-rhombohedral phases can not be distinguish due to fact that the maximum of the Bragg diffractions groups (100) and (110) are very wide. This effect is produced by very large sized grains in the PZT thin films¹⁴. In Figure 1 (c) the maximum diffraction peaks from perovskite phase are more intense when the temperature of the heat treatment is increased. The crystallization on the film increases. The peaks related to the inter-phase pyrochlore are becoming very small due to the progressive transformation to the perovskite phase.

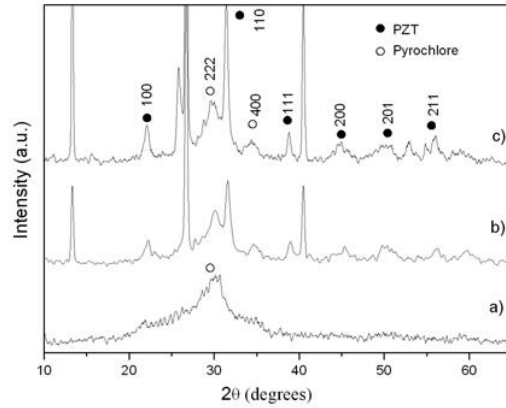


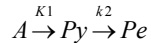
Figure 1. X-Ray diffraction patterns recorded for PZT: Eu³⁺ thin films annealed 1 h at a) 500° C, b) 550° C and c) 600° C.

Table 1 contains the positions of the maximum peaks of the different phases.

Table 1. Position peaks of pyrochlore, PbO tetragonal and PZT structures.

Phase	Position (maximum)	Position (maximum)	Position (maximum)
Pyrochlore	29.55°(222)	34.20°(400)	
PbO Tetragonal	28.65°(101)		
PZT	22.2°(100)	30.94°(101)	31.31°(110)

The formation process of the perovskite phase in the PZT: Eu³⁺ thin film is defined by the next route:



where A is the amorphous phase, Py is the pyrochlore phase and P is the perovskite phase. A heat treatment a higher temperature lets to obtain a perovskite phase well-defined.

Figure 2 shows the XRD patterns for PZT:Eu³⁺ bulk samples (pellets) doped with 0.45 molar concentration of zirconium which corresponds to the tetragonal crystalline structure.

The poor peaks observed in the Figures 2 (a) and (b) suggested an amorphous structure in the sample. The pyrochlore phase from (200) and (400) peaks can not be defined when the sample was annealed at 400° C (Fig. 2 (b)). For heat treatment at 500° C, the peaks at $2\theta = 30.94^\circ(101)$ and $2\theta = 31.39^\circ(110)$, correspond to perovskite phase. When the temperature increases, these peaks are very intense. At 700° C the reflections (100), (110), (200) and (211) are splitted corresponding to the tetragonal PbO crystalline phase. The inset in the Fig. 2 shows the low intense reflections (222) and (400) from pyrochlore-type PZT structure.

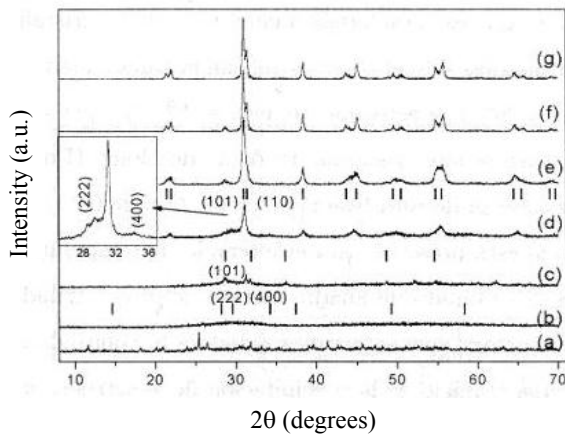


Figure 2. X-Ray diffraction patterns recorded for PZT: Eu³⁺ bulk samples (a) no heat treatment and annealed at (b) 200° C, (c) 400° C, (d) 500° C, (e) 700° C, (f) 900° C and (g) 1000° C for 1 h.

Emission and Excitation Spectra. This section shows the emission and excitation spectra from thin films and bulk samples at different temperatures. We focus on the luminescent response of the impurity Eu^{3+} inside the PZT.

i) PZT: Eu^{3+} thin film

Eu^{3+} ion was excited at 394 nm, this excitation corresponds to the $^4F_0 \rightarrow ^5L_6$ transition. Figure 3 (Left) shows the emission spectra of PZT: Eu^{3+} thin film. Before the heat treatment, the film shows a strong luminescence at 586 nm and 612 nm, which correspond to $^5D_0 \rightarrow ^7F_{1,2}$ transition from the europium. The $^5D_0 \rightarrow ^7F_3$ transition is located at 650 and $^5D_0 \rightarrow ^7F_4$ is at 701 nm. After, the film received a heat treatment of 500° and its luminescent response decreases almost completely. Emission spectrum of the thin film annealed at 500 °C shows maxima at 584 nm, 608 nm, 651 nm and 713 nm (see Fig. 3 (b)). The luminescent response is very weak in comparison to the previous signal of the thin film without heat treatment. The intensity ratio of the maxima at 608 nm ($^5D_0 \rightarrow ^7F_1$) and 651 nm ($^5D_0 \rightarrow ^7F_2$) is 0.5 in the sample without heat treatment and after 500 °C this ratio is 0.8 approximately. This increment is probably due to a possible change on the symmetry site, that can be associated to a local change of the electric field produced by the evolution of the microstructure¹⁵. After the heat treatment at 600° C, a recovery of the luminescent signal was detected.

Figure 3 (Right) shows the excitation spectrum ($\lambda_0 = 650$ nm) obtained at room temperature in the sample without treatment. This spectrum shows an intense broad band observed around 284 nm (charge transfer states (CTS)) and several low intensity bands at 394 and 460 nm due to $^7F_0 \rightarrow ^5L_6$ and $^7F_0 \rightarrow ^5D_2$ transitions, respectively. The emission spectra excited via the CTS ($\lambda_{\text{exc}} = 250$ nm) are shown in Figure 4. Figure 4 (d) shows the initial spectrum (no heat treatment) with some bands at 588 nm, 612 nm, 649 nm and 693 nm, which correspond to the $^5D_0 \rightarrow ^7F_{1 \rightarrow 4}$ transition, where 7F_2 is a hypersensitive transition.

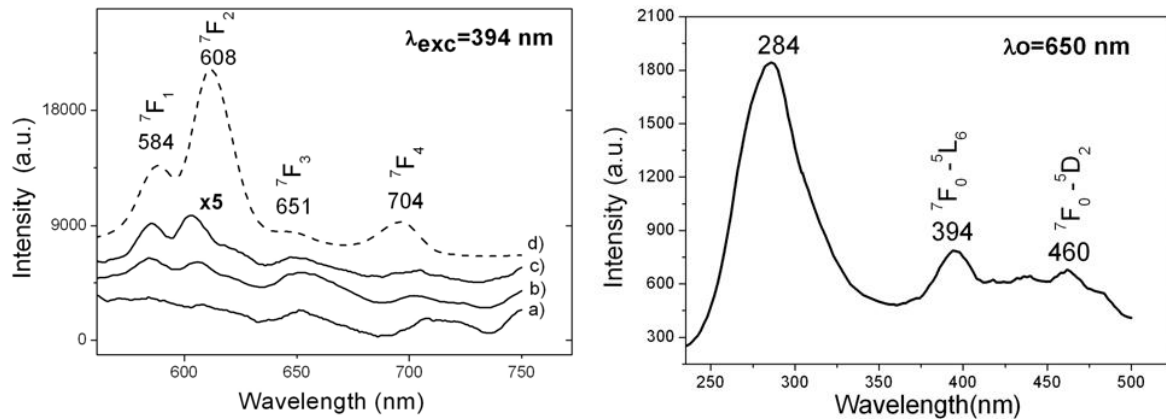


Figure 3. Left: Emission spectra of Eu^{3+} in PZT thin film by using $\lambda_{\text{exc}} = 394$ nm (samples annealed 1 h at different temperatures) a) 500° C, b) 550° C, c) 600° C and d) No heat treatment. Right: Excitation spectrum observed at $\lambda_0 = 650$ nm.

Figure 4 (a) contains the luminescence spectrum of film annealed at 500° C, and no peaks were observed from main transitions. Figure 4 (b) shows a little recovery of the luminescence, and the $^5D_0 \rightarrow ^7F_{1,2}$ transitions can be detected with similar intensity. Finally, in Figure 4 (c) from thin film annealed at 600° C, the luminescence increase and the $^5D_0 \rightarrow ^7F_{1,2}$ transitions can be observed.

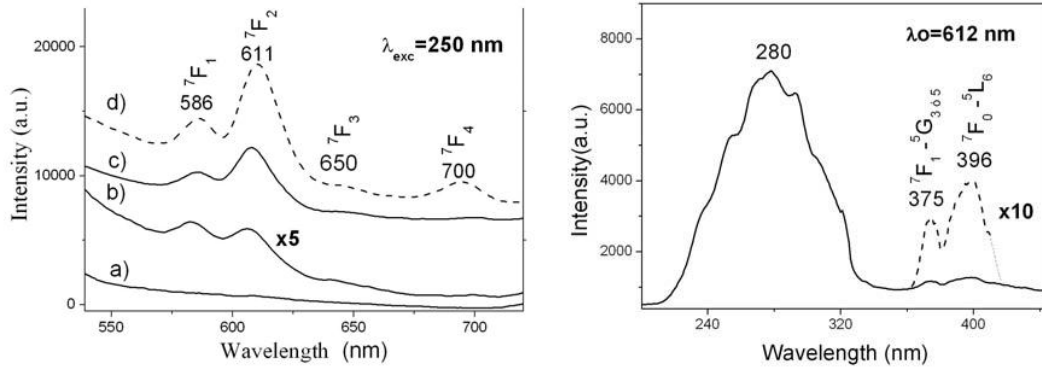


Figure 4. Left: Emission spectra of Eu³⁺ in PZT thin film by using $\lambda_{exc} = 250$ nm (at different temperatures a) 500° C, b) 550° C, c) 600° C and d) No heat treatment. Right: Excitation spectrum observed at $\lambda_0 = 612$ nm.

Figure 4 (Left) shows the excitation spectrum ($\lambda_0 = 612$ nm) of the thin film. A broad band is centred at 280 nm. Two weak peaks located at 375 nm y 396 nm, corresponding to the ${}^7F_0 \rightarrow {}^5L_6$ y ${}^7F_1 \rightarrow {}^5D_3$ transitions, are observed. The relative intensity o this spectrum is bigger than that from excitation spectrum observed at $\lambda_0 = 650$ nm. Literature mentions this effect indicating that the luminescent response is dominated by the red emission at 612 nm, which corresponds to the ${}^5D_0 \rightarrow {}^7F_2$ transition¹⁶.

ii) Bulk sample

Figure 5 (Left) shows the emission spectra from PZT: Eu³⁺ bulk sample exciting at $\lambda_{exc} = 394$ nm. Before heat treatment the bulk sample exhibit a strong luminescent response located in the peaks at ${}^5D_0 \rightarrow {}^7F_{1,2}$ transitions mainly. After, the spectrum of the sample annealed at 200° C shows low intense peaks which disappear when the sample was annealed at 300° C. This inhibition of the luminescence when the sample is annealed by heat treatment is systematic and could be associated wit the crystallite size formed in the samples during crystallization and the recovery is due to the confinement of the impurity^{17,18}. Same interpretation is possible for the thin film behavior. The luminescence is recovered when the sample is annealed at 1000° C.

Figure 5 (Right) shows the spectra by exciting through the ${}^7F_0 \rightarrow {}^5L_6$ transition at 395 nm (emission), and observing at 652 nm (excitation). The excitation spectrum exhibits a CTS broad band observed in the previous spectrum. The broad bands are $f-f$ transitions, and the most intense corresponds to ${}^7F_0 \rightarrow {}^5L_6$ transition. In the emission spectrum, some peaks associated to the relaxation to the ${}^7F_{1-4}$ states from 5D_0 state are observed.

Electronic Decays and Lifetimes. Figure 6 shows the decay curve of lifetime from ${}^5D_0 \rightarrow {}^7F_1$ emission when exciting at the 5L_6 in the PZT:Eu³⁺ thin film. The electronic decays show two general components: a fast one and a slow one. The experimental data were fitted by using a double exponential expressed by the next equation:

$$y = A1 \cdot \exp(-x/t1) + A2 \cdot \exp(-x/t2) + y0$$

Table 2 shows these components.

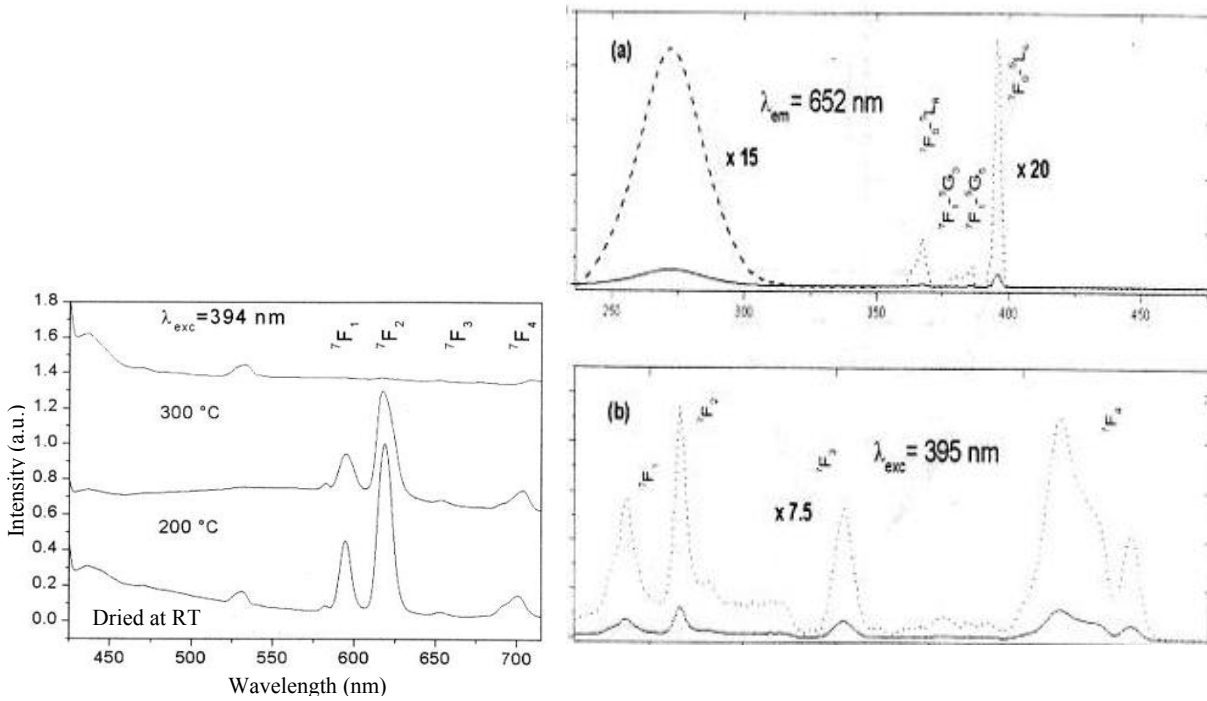


Figure 5. (Left) Luminescence evolution by exciting at $\lambda_{exc} = 394$ nm after heating the samples 1 h at different temperatures. (Right) Excitation spectra observed at $\lambda_o = 652$ nm and emission spectra at $\lambda_{exc} = 395$ nm.

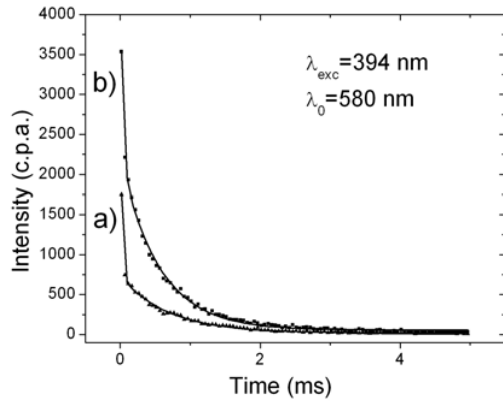


Figure 6. Electronic decay by exciting at $\lambda_{ext} = 394$ nm and observing at $\lambda_o = 580$ nm: a) Thin film annealed at 550 °C, and b) No heat treatment.

Tabla 2. Components of the electronic decays for the thin films.

	Fast component (ms)	Slow component (ms)	Correlation coeff.
No heat treatment	0.09336 \pm 0.001879	1.20632 \pm 0.18722	0.99779
Annealed at 550 °C	0.03598 \pm 0.00651	1.3333 \pm 0.26517	0.99742

In the case for thin film annealed at 550 °C, the slow component is two times bigger than those observed at 280 nm without heat treatment and it is 1.5 times bigger when the sample was annealed at 550 °C.

Figure 7 shows the decays slopes of the lifetimes from a bulk sample by exciting at 245 nm and 394 observed at 616 nm in both cases. When the sample is exciting at 394 nm through the 5L_6 level, the lifetime is six times bigger than

that obtained by CTS (245 nm). This is a proof of the transitions exciting through the CTS band are more possible than those exciting at the $f-f$ levels directly. Table 3 shows the slow and fast components.

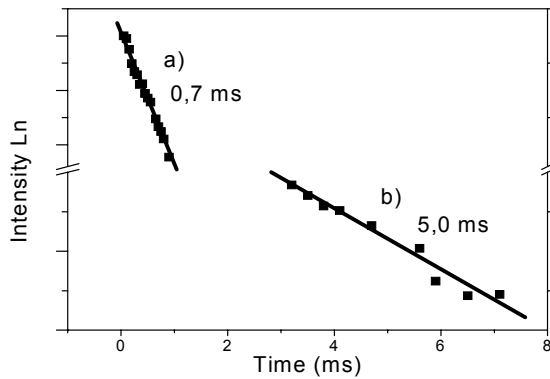


Figure 7. Lifetimes of PZT bulk sample by exciting at a) $\lambda_{\text{exc}} = 245$ nm and, b) $\lambda_{\text{exc}} = 396$ nm. Both spectra were observed at $\lambda_0 = 616$ nm.

Table 3. Fast and slow components

Fast component ${}^7F_0\text{-BTC-}{}^5D_0$	Slow component ${}^7F_0\text{-}{}^5L_6\text{-}{}^5D_0$
0.7 ms	5.0 ms

4. CONCLUSIONS.

Excellent PZT: Eu^{3+} sol-gel thin films were obtained showing a crystalline structure, *perovskite*. A PZT pyrochlore phase appears in conjunction of the crystallization. The *perovskite* phase detected in the thin films was obtained at lower temperature than that from bulk samples. This is a very important technological fact because the preparation of the thin films doped with some impurity is faster than the bulk samples. Luminescence studies were done in both samples. The luminescent response of the europium Eu^{3+} ion was loss when the sample was annealed at 500 °C. But, the luminescent signal was recover at 600 °C. The evolution of the luminescent response can be followed at 550 °C. The response of the hypersensitive transition (612 nm) dominates the emission. A broad CTS band was observed in the excitation spectra and narrow peaks produced by the ${}^7F_0 \rightarrow {}^5L_6$ y ${}^7F_1 \rightarrow {}^5D_3$ transitions exciting at $\lambda_o = 612$ nm, others peaks produced by ${}^7F_0 \rightarrow {}^5L_6$ y ${}^7F_0 \rightarrow {}^5D_2$ transitions exciting at $\lambda_o = 650$ nm. The excitation by CTS is more intense than through $f-f$ levels. Eu^{3+} can work as structural probe to determine the matrix structure. The electronic decays possess two general components: a fast one and slow one.

In the bulk samples, a good perovskite phase was obtained at 500° C. PZT pyrochlore phase was no found. A tetragonal phase in conjunction the crystallization was identified. The perovskite phase was obtained in samples annealed at higher temperatures than those used in the thin films. An inhibition of the luminescence was registered at 300° C, but this response was recovered at 1000° C. This inhibition is associated to the nanocrystals formed in the bulk sample. Hypersensitive transitions as ${}^7F_0 \rightarrow {}^5D_2$ (excitation) or the ${}^5D_0 \rightarrow {}^7F_2$ (emission) were observed. These transitions indicate that the Eu^{3+} occupies a low symmetry site. The lifetimes of the emission exciting through 5L_6 and through CTS band (245 nm) are 5 ms and 0.7 ms, respectively. It proves that the transition is less prohibited when exciting through the CTS. The transition probabilities in the thin films are bigger than those from bulk samples.

ACKNOWLEDGEMENTS

This work has been supported by the following grants: CONACYT 43226-F, NSF-CONACYT, ECOS M02-P02 and PAPIIT 116506-3.

REFERENCES

1. Rui M. Almeida, A. C. Marques *Journal of Non-Crystalline Solids* 352, 475–482 (2006).
2. S. B. Majumder, B. Roy, R. S. Katiyar and S. B. Krupanidhi *J. Appl. Phys.* 90, 2975 (2001).
3. A. Garg and D. C. Agrawal 2001 *Mater. Sci. Eng.* B 86 134.
4. A. Garg and T. C. Goel *Mater. Sci. Eng.* B 60, 128 (1999).
5. S. R. Shannigrahi, R. N. P. Choudhary and H. N. Acharya *Mater. Res. Bull.* 34, 1875 (1999).
6. S. R. Shannigrahi, R. N. P. Choudhary and H. N. Acharya *J. Mater. Sci. Lett.* 18, 345 (1999).
7. L. Pintilie and I. Pintilie *Mater. Sci. Eng.* B 80, 388 (2001).
8. C. Lee, V. Spirin, H. Song and K. No *Thin Solid Films* 34, 242 (1999).
9. G. Teowee, J. M. Boulton, E. K. Franke, S. Motakef, T. P. Alexander, T. J. Bukowski and D. R. Uhlman *Integr. Ferroelec.* 15 281 (1997).
10. F. González, P. Schabes-Retchkiman and J. Garia-Macedo *J. Phys. D: Appl. Phys.* 37, 2442–2445 (2004).
11. Yi G, Wu Z and Sayer M *J. Appl. Phys.* 64, 2717 (1988).
12. Angus P. Wilkinson, James S. Speck, and A. K. Cheetham', *Chem. Mater.*, 6, 750-754 (1994).
13. K. Nomura, Y. Takeda, M. Maeda and N. Shibata *Jpn. J. Appl. Phys.* 39 5247-5251 (2000).
14. R. W. Schwartz, J. A. Voigt, and B. A. Tuttle, *J. Mater. Res.*, 12, 444-456 (1997).
15. Q. Zhong, L. Cun, Z. Ning *J. Lumin.* 99, 29-34 (2002).
16. H.X. Zhang, Y. Zhou, C. Kam, Y. Lam, Y.C. Chan, *Mat. Res.* 560 9-14 (1999).
17. W. Chen, A. G. Joly, C.M. Kowalchuk, J.O. Malm, Y. Huang, J. Bovin *J. Phys. Chem. B* 106 7034 (2002).
18. F. Gonzalez, P. Schabes, J. Garcia, *J. Phys. D: Appl. Phys.* 37 2442-2445 (2005).